Geological Magazine

www.cambridge.org/geo

Discovery of concealed copper orebodies at the Deerni copper deposit, northwest China by integrated geological investigations

Xi-An Yang[1], Jie Wu[2] and Deru Xu[1]

[1]State Key Laboratory of Nuclear Resources and Environment, East China University of Technology, Nanchang, China and [2]School of Environment, University of Auckland, Auckland, New Zealand

Original Article

Cite this article: Yang X-A, Wu J, and Xu D. Discovery of concealed copper orebodies at the Deerni copper deposit, northwest China by integrated geological investigations. *Geological Magazine* **162**(e28): 1–15. https://doi.org/10.1017/S0016756825100083

Received: 22 February 2024
Revised: 10 May 2025
Accepted: 30 May 2025

Keywords:
Concealed orebody; copper deposit; Deerni; ore-controlling structure; mineral exploration

Corresponding authors: Xi-An Yang; Email: yangxianyantai@163.com, Deru Xu; Email: xuderu@ecit.cn

Abstract

The Deerni copper deposit is one of the largest in Qinghai province, China, with proven copper reserves of 0.556 Mt. To explore new copper orebodies, we conducted a geological study at western Deerni focusing on hydrothermal alterations and ore-controlling structures. Field investigation shows that the deposit is hosted mainly within the central segment of the Deerni ophiolite. Additional hosts include Lower-Permian slate, limestone, gabbro and volcanic rock, as well as the contact zone between granite and slate. Such observations indicate that the Deerni copper deposit is not only associated with the ophiolite, but its formation is also controlled by faults. Alterations including serpentinization, carbonatization, silicification and malachite, and magnetite mineralization occurred along fractures within the wall rocks and surrounding strata. This means the alteration post-dated structural activity that affected the Lower Permian strata in the region. The Deerni copper deposit is controlled by the NW-striking faults. This is evidenced by (1) slate fragments and breccias within the orebodies, (2) saw-toothed boundaries between the orebodies and host rocks, (3) copper ore veinlets and (4) striations and step patterns on the orebody surface and hanging-wall-hosted quartz veins. Mineralization controlled by NW-trending faults suggests a major orebody ('No. 2') likely extends to either northwest or southeast. Field investigations along with geophysical and geochemical data, thus predicted the presence of concealed copper orebodies in western Deerni. Subsequent drilling projects have verified this prediction and revealed three concealed orebodies with widths of 7.15–13.87 m and Cu grade of 1.00–11.34 wt.%, adding 10,000 tonnes to the copper reserves.

1. Introduction

The Deerni copper deposit is one of the largest copper reserves in the Tethys metallogenic belt, with proven copper reserves of 0.556 Mt (Duan *et al.* 2014). This deposit was first discovered by a local herdsman in 1958. In 2003, the Zijin Mining Group Company Limited acquired the exploration and mining rights, commencing mining operations in 2006. After 18 years of extraction, the main copper orebodies are now nearly depleted, making the discovering of new orebodies essential to sustain the copper mining activities at Deerni (Wang *et al.* 2008).

Song *et al.* (2008) indicated that the carbonaceous Fe-Si rock within the deposit is a hydrothermal sedimentary rock. Based on local-scale geological mapping and lithological profiling, Jiao *et al.* (2009) concluded that the copper mineralization at Deerni postdates the ultrabasic rocks. Moreover, Song *et al.* (2012) interpreted the ferro-siliceous rocks at Deerni as exhalative rocks formed by submarine volcanism, suggesting an association with submarine exhalative-sedimentation. Based on those features, Deerni was classified as a deposit of volcanogenic massive sulphide (VMS) type and subjected to extensive exploration efforts including geochemical and geophysical surveys, as well as exploratory drilling (Zhang, 2014). However, new copper orebodies have yet to be discovered.

Some researchers have proposed a magmatic origin for the Deerni copper deposit. Zhang *et al.* (1995, 1996) suggested that the deposit represents a magmatic sulphide deposit, and the mineralization is contemporaneous with the ultrabasic host rocks and controlled by faulting. Duan (1996, 1998) argued that it is a hydrothermal deposit related to the emplacement of Indosinian granite intrusions. They suggested that the ore-forming materials were sourced from both Indosinian granitic magma and Late Paleozoic slate. These researchers also noted that faults bound the deposit and that pyrite occurs sporadically throughout the Indosinian granite, just north of the main Deerni deposit.

The debate over whether the Deerni copper deposit is primarily related to local volcanism or magmatism has persisted for decades. The need to discover new orebodies has revitalized interest in re-examining the source and genesis of the deposit, to refine the prospecting model and guide future exploration efforts.

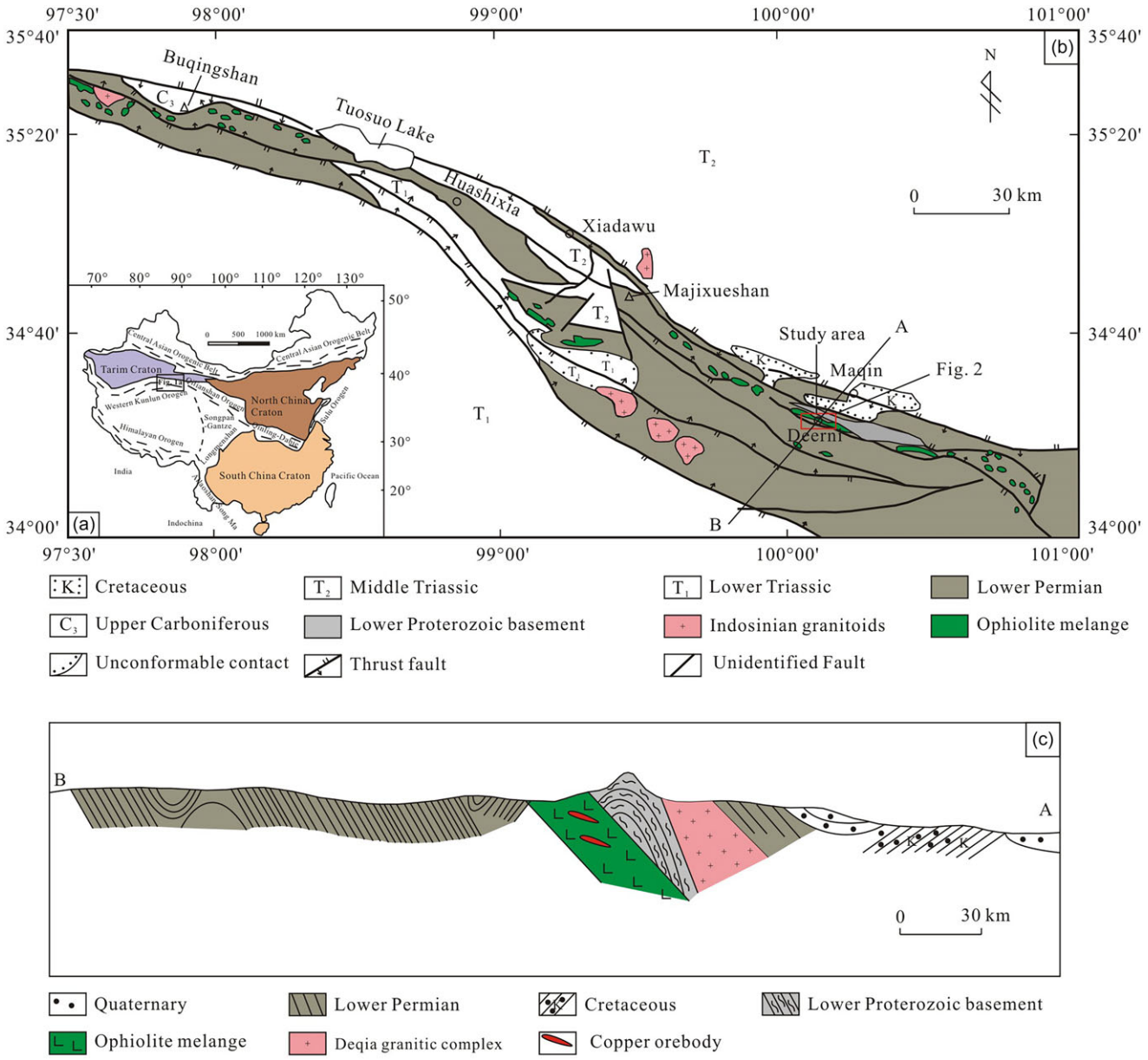

Figure 1. (a) Schematic tectonic map of China (modified from Zhao & Guo, 2012); (b) Geological sketch map of the eastern part of the Animaqin tectonic belt, NW China (modified from Yang *et al.* 2005), with the Deerni study area outlined in a red rectangle; (c) A-B profile of the Animaqin tectonic belt (modified from Duan, 1991).

By integrating geological, geochemical and geophysical data, we propose a new model for the copper mineralization processes at the Deerni copper deposit. Our findings provide new insights into the deposit's formation and contribute to the development of a more effective exploration strategy for discovering concealed orebodies.

2. Geological background

The Deerni copper deposit is located within the eastern segment of the Animaqin tectonic belt. Intense compression in this belt has resulted in the fragmentation of rock units and the extensive development of complex geological structures (Fig. 1). These fragmented strata form a mélange, with disordered stratigraphic units (Chen *et al.* 1999, 2000*a*, 2001). The outcropping rocks in the Deerni copper deposit span Paleozoic, Mesozoic and Cenozoic eras (Fig. 2). The Paleozoic rocks, found in northern Deerni, are in faulted contact with the Deerni ophiolite. These rocks are ~670 m thick, comprising amphibolite (SHRIMP U-Pb zircon age at 417.11 ± 3.3 Ma, Yang *et al.* 2005) and interlayered marble, along with banded tremolite marble.

The Upper Carboniferous marine clastic and carbonate rocks strike northwest-southeast and dip northeast. The lower portion of this formation is ~490 m thick and consists of interbedded meta-sandstone, meta-conglomerate, andesite and lenticular limestone. The upper section (~430 m thick) is characterized by bioclastic and crystalline limestone with thin sandstone beds. This sequence is unconformably overlain by Lower Permian rocks (Yang *et al.* 2005).

The Lower Permian strata also strike northwest-southeast, with thickness varying from several to tens of metres along strike. They comprise interlayered fine-grained sandstone and slate, as well as lenses of greyish-green meta-andesite and fossiliferous limestone.

https://doi.org/10.1017/S0016756825100083 Published online by Cambridge University Press

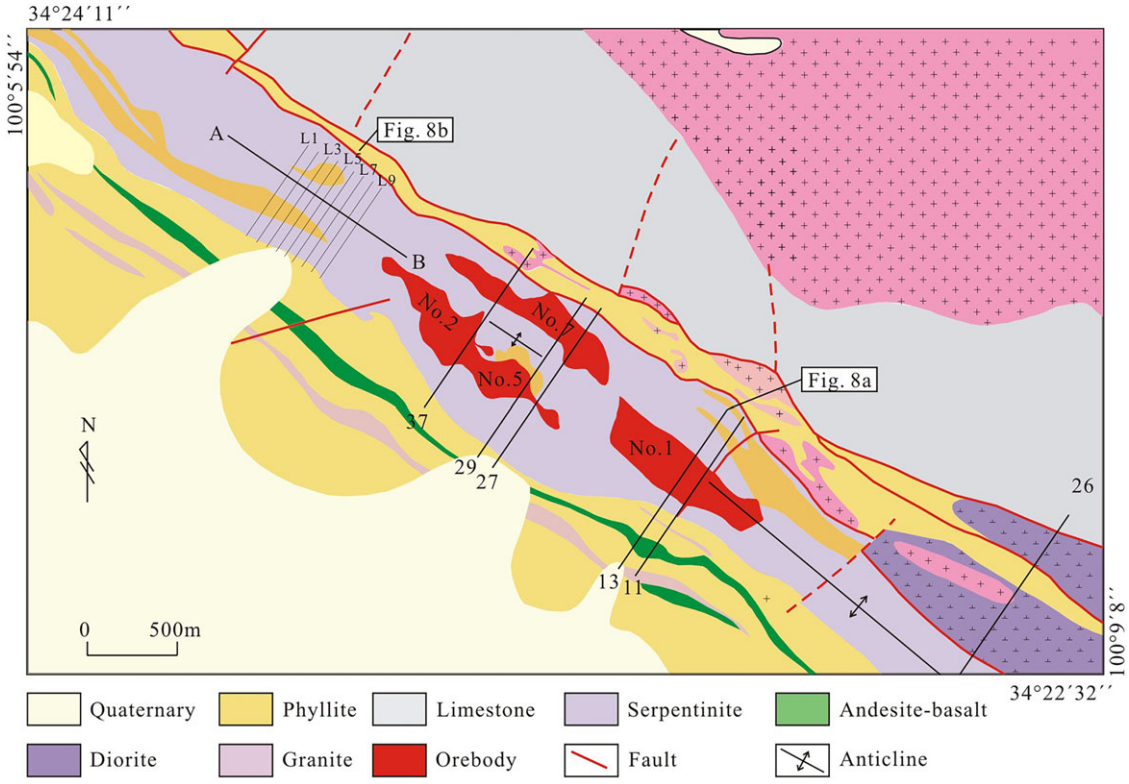

Figure 2. Geological sketch map of the Deerni copper deposit (modified from Guo *et al.* 2024).

These strata are interbedded with tectonically dismembered fragments of the Deerni ophiolite, creating a mélange that includes abyssal mudstone and radiolarian chert (Fig. 2). Near the Deerni copper deposit, the Lower Permian slate (>400 m in thickness) is hosted within the ophiolite.

The Upper Permian strata, located to the north of the Upper Carboniferous, consist of interbeds of grey fossiliferous limestone and fine-grained yellow sandstone. Early to Middle Jurassic rocks include sandstone and sandy shale, with carbonaceous shale containing fossils interbedded with limestone lenses and coal beds, which are directly overlain by conglomerate (Yang *et al.* 2005).

Cretaceous rocks cropping out in the northern part of the study area are composed of amaranth conglomerate, sandy conglomerate and thin layers of very fine-grained sandstone containing fossil plant remains and trace fossils. The conglomerate features detrital grains and rock fragments of limestone, sandstone, slate, andesite and granite, with grains cemented by calcite and micritic calcite (Yang *et al.* 2005).

The Deerni ultrabasic rocks exhibit characteristics typical of ophiolites, leading to their classification as the Deerni ophiolite (Yang *et al.* 2009). This dismembered ophiolite is typically exposed as blocks of varying sizes within a sheared flysch matrix, striking northwest-southeast (Chen *et al.* 1999, 2000*a*, 2001, 2004; Pan *et al.* 2012). The ophiolite extends over ~80 km with a width of 10 to 20 km (Yang *et al.* 2009), consisting of meta-peridotite, basaltic lavas, mafic-ultramafic cumulates and sheeted dykes. The peridotite includes dunite, harzburgite, lherzolite, feldspathic lherzolite and garnet lherzolite. The Deerni ophiolite has been dated to 345.3 ± 7.9 Ma using ^{40}Ar-^{39}Ar method (Chen *et al.* 2001), slightly older than the zircon SHRIMP U-Pb age of 308.0 ± 4.9 Ma (Yang *et al.* 2009). It is considered to represent fragments of subducted oceanic crust, providing evidence for sea-floor spreading during the middle to late Carboniferous, when the Paleo-Tethyan Ocean began to break apart (Yang *et al.* 2009).

Several Indosinian granitic intrusions are located along the northern margin of the Deerni ophiolite (Fig. 2). The largest of these is the Deqia granitic complex, with a zircon SHRIMP U-Pb age of 250 ± 20 Ma (Yang *et al.* 2005). This complex extends 16 km in length and 100 to 200 m in width, consisting primarily of weakly deformed and metamorphosed granite, with minor granodiorite and quartz diorite. It intruded into Paleozoic amphibolite and marble and locally cuts through the Deerni ophiolite. The complex is unconformably overlain by Early to Middle Jurassic sandstone and conglomerate along its northern edge and by Pliocene sedimentary rocks to the west (Yang *et al.* 2005).

The Deerni copper deposit (latitude: 34°23′7″N, longitude: 100° 07′15″E) is situated in the central part of the Deerni ophiolite (Wang & Qin, 1989). The ophiolite serves as the primary host for copper orebodies (Fig. 1c), although some orebodies are also found within Lower Permian slates. The region has experienced significant magmatic activity, leading to the formation of mafic-ultramafic, intermediate-acidic and dike rocks (Guo *et al.* 2024). Ultramafic rocks are concentrated in the central part of the deposit, forming a belt 70–800 m wide that gradually narrows as it extends beyond the mining area (Tang *et al.* 2024). The peridotite has been extensively altered to serpentinite, obscuring its original structure. Slate and phyllite host the ultramafic rocks and occur as xenoliths. The Deerni deposit is intersected by NW-SE and NE-SW faults. Due to the prevalence of ultramafic rocks, fold structures are difficult to discern, though the fold axis appears to align with the strike of the ultramafic rocks. A syncline is adjacent to an anticline on both the southern and northern sides (Fig. 1c), with the

https://doi.org/10.1017/S0016756825100083 Published online by Cambridge University Press

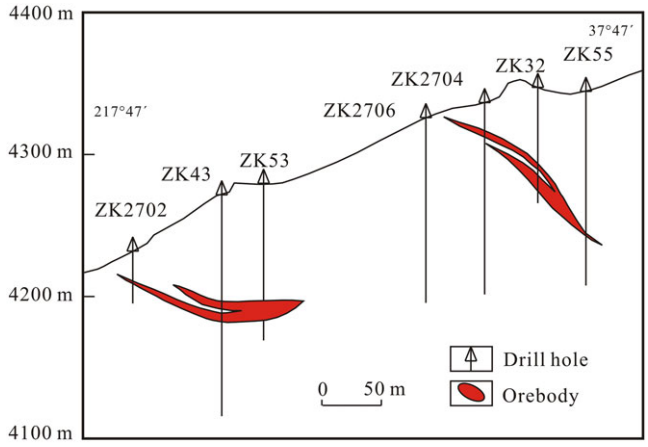

Figure 3. Number 27 cross-section through the Deerni copper deposit (based on unpublished data from the Zijin Mining Group Company Limited, 2015).

orebodies located within the anticlinal core. The anticline structure is prominent between exploration lines 11–26 and 29–37, but becomes less distinct or disappears towards the east and west.

The main orebodies currently being mined include No. 1, 2, 5 and 7 (Fig. 2), located between elevations of 3990 and 4390 m (Fig. 3). These orebodies extend 460–1060 m along strike, with an average width of 88–193 m and depths ranging from 190 to 320 m. The orebodies frequently exhibit boudinage or folding, displaying lenticular shapes, with distinct boundaries between the ore and the wall rocks. Hydrothermal alteration is extensive, characterized by serpentinization, carbonatization, silicification and malachite alteration, as well as magnetite mineralization. Serpentinization and carbonatization are the most common alteration types. Serpentinization involves the replacement of olivine and pyroxene by serpentine, and carbonatization is evident in quartz-calcite veins within the surrounding rocks. Minerals resulting from carbonate alteration include calcite, dolomite and magnesite.

The main ore types are classified as massive, vein and breccia ores. Massive ores are primarily composed of sulphides (60–80%), silicates (20–40%) and oxides (5–10%). Veinlet ores, typically 5–30 cm in width, often traverse serpentinite country rocks or massive ores, while breccia ores are characterized by serpentinite clasts cemented by hydrothermal minerals and sulphides. The ores contain 0.64–1.64 wt.% Cu, 0.053–0.17 wt.% Co and 0.65–7.28 wt.% Zn. Ore minerals include pyrite, chalcopyrite, sphalerite, pyrrhotite and magnetite, along with subordinate galena, hengleinite, ilmenite and leucosphenite. Gangue minerals comprise quartz, calcite, rutile, fluorite and zircon. Oxidized ore consists of limonite, tenorite, malachite and azurite, with oxidized ores typically found at the surface and sulphide-rich ores at deep levels.

The ores exhibit a range of textures, including euhedral, anhedral, granular, fractured and pore-filling textures, as well as massive, disseminated, brecciated and veinlet structures. Based on the relationships among ore intersections, structures and mineral assemblages, the Deerni deposit can be categorized into four mineralization stages (Duan, 1991).

3. Methods

Comprehensive fieldwork was conducted at the Deerni copper deposit to investigate hydrothermal alterations and the structural characteristics of the deposit.

Fault and fracture attitudes were measured using a compass clinometer. The conjugate joint sets identified in both the wall rocks and copper orebodies were subjected to statistical analysis. Structural geology and CAD software were utilized to create stereographic projections of the measured structures (Yang *et al.* 2020, 2023) to determine the compression direction and kinematic features of the structures within the copper deposit. This statistical analysis of the conjugate joint sets provided insights into the compression direction and the ore-controlling structural characteristics at the Deerni copper deposit.

Contour maps serve as effective tools for illustrating the spatial distribution of geological bodies and are widely employed in mineral exploration. They are particularly useful for identifying geochemical and geophysical anomalies, as well as for structural studies (Yang *et al.* 2020, 2023). Most drilling activities in the western part of Deerni were completed; so, relevant samples and data from Zijin Mining Group Co., Ltd. were accessed for this study. Contour maps and surface trend maps were generated using Surfer 11 software.

The geographical and geochemical survey of western Deerni has been completed, magnetic, gravity and self-potential anomaly patterns, transient electromagnetic anomaly profile, and distribution pattern of Cu–Pb–Mn–Ni mineralization at western Deerni were obtained from Zijin Mining Group Co., Ltd. for this study.

The original magnetic field dataset covers an exploration area of 18.2 km^2, which occupies the vast majority of the Deerni Copper Mine area. The data exist in grid format with a grid size of approximately 100 m × 20 m. The magnetic survey comprises a total of 9,283 measurement stations, covering a cumulative survey line length of 182 km. In addition, seven magnetic survey profiles were completed, containing a total of 692 measurement stations.

In 1992, the Third Brigade of the Non-ferrous Geophysical Team conducted a 1:20,000 gravity survey in the area from western Deerni mine to Zhabenggou. A total of eight gravity anomalies were identified, with some exhibiting considerable scale and broadly coinciding with known orebodies.

During the early exploration phase of the Deerni copper deposit, the self-potential method achieved remarkable success in mineral targeting. In 1990, the Third Brigade of the Non-ferrous Geophysical Team conducted a 1:10,000-scale self-potential survey grid within the mining area and its periphery, covering a cumulative area of 52 km^2. A total of 28 self-potential anomalies were identified, with 14 confirmed as mineral-induced through follow-up verification (Wang *et al.* 2007*b*). The transient electromagnetic survey of western Deerni has been completed; relevant profiles from Zijin Mining Group Co., Ltd. were accessed for this study. There are nine transient electromagnetic surveying lines in the study area. The dimensions of the working network are 100 m × 100 m (i.e., distances between lines and points are both 100 m; Fig. 2). Due to the large-scale of ore body, shallow burial and intense topographic dissection, the migration conditions of geochemical halos are favourable. In 1990, the Second Brigade of the Non-ferrous Geophysical Team conducted a 1:10,000 scale geochemical survey work from the western Deerni mine to Zhabenggou.

4. Results

4.a. Hydrothermal alterations

Duan (1991) classified the hydrothermal alterations at the Deerni copper deposit into four distinct stages: stage 1 is characterized by serpentinization and carbonatization, with paragenetic minerals of

https://doi.org/10.1017/S0016756825100083 Published online by Cambridge University Press

Table 1. The paragenetic sequence of mineralization at the Deerni copper deposit (modified from Duan, 1991)

	Hydrothermal stage				
Minerals	Pyrite	Magnetite	Pyrrhotite	Pyrite-marcasite	Supergene stage
Pyrite	_____		_____		
Chalcopyrite	_____		_____		
Sphalerite	_____		_____		
Marcasite	_____			_____	
Magnetite		_____			
Haematite		_____			
Cubanite		_____			
Pyrrhotite			_____		
Hengleinite			_____		
Siegenite			_____		
Quartz			_____		
Carbonate	_____				
Talc	_____				
Limonite					_____
Tenorite					_____
Hausmannite					_____
Malachite					_____
Azurite					_____
Covellite					_____
Chalcocite					_____
Bornite					_____
Zigueline					_____
Native copper					_____
Native gold					_____
Chalcanthite					_____

pyrite, chalcopyrite, sphalerite, marcasite, carbonate and talcum (Table 1); stage 2 by serpentinization, carbonatization and magnetite mineralization with magnetite, haematite, cubanite, carbonate and talcum; stage 3 by silicification and carbonatization, with pyrite, chalcopyrite, sphalerite, pyrrhotite, hengleinite, siegenite, quartz and carbonate and stage 4 by primarily carbonatization with pyrite, marcasite and carbonate. In addition, the supergene stage is characterized by malachite mineralization and contains limonite, tenorite, hausmannite, malachite, azurite, covellite, chalcocite, bornite, zigueline, native copper, native gold and chalcanthite.

A detailed investigation of hydrothermal alterations in the Deerni copper deposit revealed that serpentinization (comprising talcum, antigorite and serpophite) and carbonatization (predominantly calcite, with dolomite and magnesite) occurred throughout the Deerni ophiolite. Serpentinization developed during the hydrothermal stages 1 and 2 and may be overprinted by carbonatization (Fig. 4a). Carbonatization was observed in all four stages and is commonly associated with pre-existing structures (Fig. 4b), appearing as carbonate veinlets along fractures in the ophiolite. These veinlets generally exhibit a lattice-like texture of calcite, with widths ranging from 1 to 20 mm and lengths extending up to several metres.

Magnetite mineralization, which developed during stage 2, occurs sporadically along fractures within the ophiolitic rocks (Fig. 4c) or as magnetite veinlets and may coexist with malachite.

Silicification emerged during stage 3, with two NW-striking silicified zones identified at the southern slope and the ridge (as a steep cliff) of Mount Deerni. The Deerni copper deposit is located within the silicified zone at the southern slope, where silicification is the most intense in the orebodies and diminishes in the surrounding wall rock. Silicified lenses and bands, along with quartz veinlets, are found in both the ophiolite and slate throughout the upper parts of the copper orebodies (Fig. 4d), measuring several to tens of metres in width and tens to hundreds of metres in length. Silicification mainly comprises quartz deposition along vesicles and fractures, resulting in an earthy to yellow rock surface with a grey to white interior. Along the ridge of Mount Deerni, the extent of silicification in the ophiolite varies along strike. The average Cu grade in the ophiolite is 0.0024 wt.% (Table 2), while the average Cu grade in silicified ophiolites is 0.105 wt.%. Ten silicified ophiolite samples show Cu grades ranging from 0.004 to 0.061 wt.% (Table 2).

Malachite mineralization developed during the supergene stage, with joints within the Deerni copper deposit displaying green and blue-green surfaces indicative of malachite and/or azurite copper

https://doi.org/10.1017/S0016756825100083 Published online by Cambridge University Press

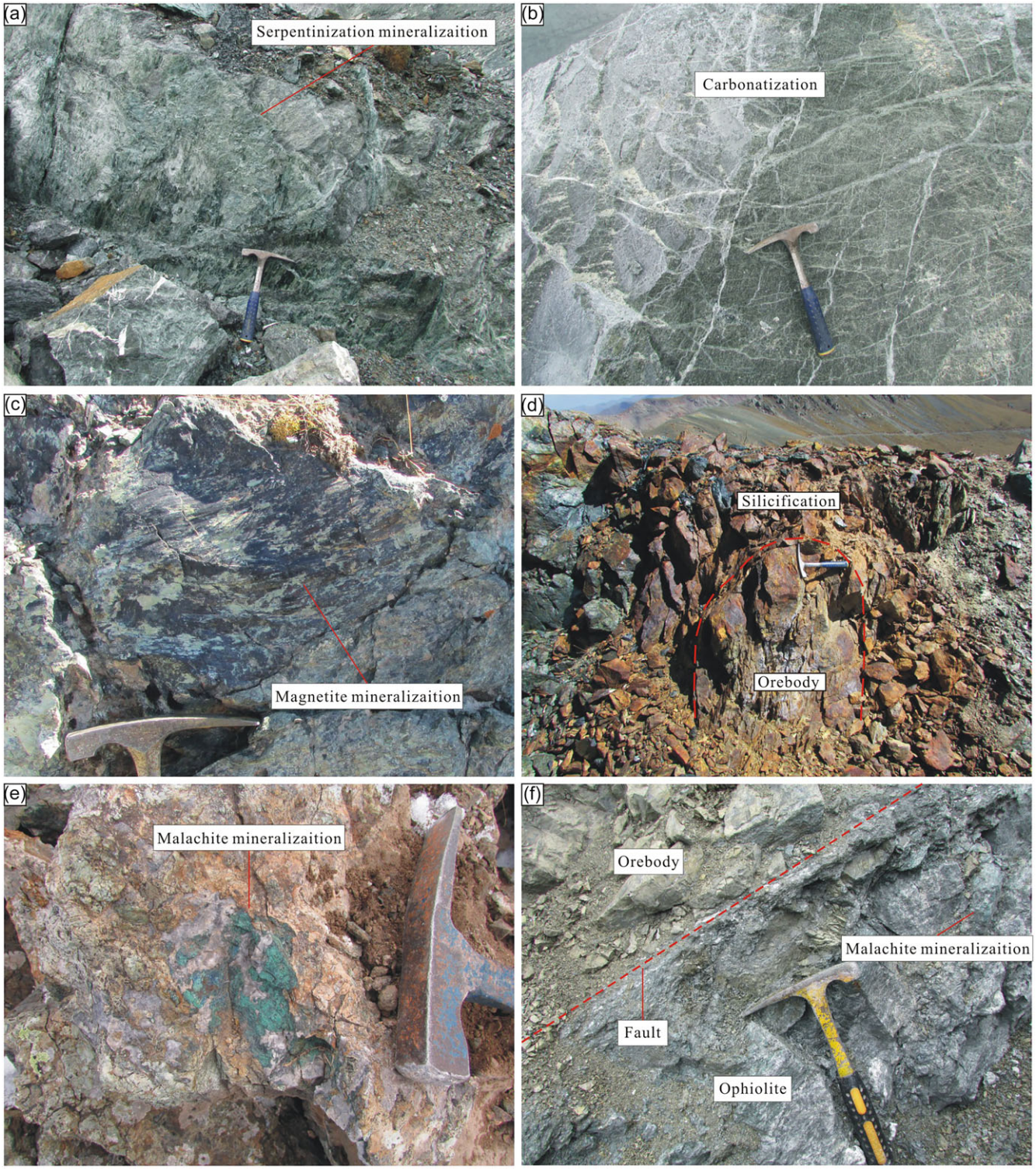

Figure 4. Outcrop photographs of different types of hydrothermal alteration at the Deerni copper deposit: (a) Serpentinization occurring in the ophiolite on both sides of the copper orebodies; (b) Carbonatization occurring along fracture surfaces on both sides of the copper orebodies; (c) Magnetite occurring as veinlets in fractures within the ophiolite; (d) Silicification mainly occurring in the upper parts of the copper orebodies; (e–f) Malachite principally occurring along fracture surfaces on both sides of the copper orebodies.

mineralization. Malachite typically appears along fracture surfaces in altered ophiolite, on either side of the copper orebodies (Fig. 4e and f). It also occurs as patches within the siliceous cap, as stains along the cleavages of magnetite-bearing altered ophiolite, and as coatings on fractured outcrops of granite dykes.

4.b. Ore-controlling structures and determination of paleo stress directions

The Deerni copper deposit is located in the anticlinal core (Fig. 1c) and is clearly influenced by faults, with orebodies bordered along

https://doi.org/10.1017/S0016756825100083 Published online by Cambridge University Press

Table 2. The elements content in the wall rocks and copper orebody at the Deerni copper deposit

		Cu (%)	Ni (%)	Cr (%)	Co (%)	Pb (%)	Data source
Ophiolite	Average	0.0024	0.18	0.13	0.0079		Liu *et al.* 2007
Silicified Ophiolite	Number of samples	10					This study
	Range	0.034~0.27					
	Average	0.105					
Slate	Average	0.0040	0.0031	0.0091	0.0011	0.0014	Liu *et al.* 2007
Upper Carboniferous schist	Average	0.0267	0.0097	0.008	0.0044	0.00035	
Granite	Average	0.0022	0.0019	0.0032	0.0016	0.0022	
Ore	Number of samples	38	38	38	38	38	Song *et al.* 2007
	Range	0.2~3	0.002~0.1	0~0.07	0.003~0.05	0~0.01	
	Average	0.97	0.025	0.015	0.019	0.0038	

Table 3. Characteristics of ore-controlling structures at the Deerni copper deposit

Structures	Structural characteristics			Geological significance
Ore-controlling structures	Wall rocks	Deerni copper deposit	Ophiolites and slates	It implies the final body has been structurally deformed. Consider remobilization after ore formation.
		Deerni copper area	Gabbro, limestone, the contact zone between granite and slate, volcanic rocks	
	The boundary between the orebodies and the wall rocks is sharp			It implies the orebody was controlled by faults, and it is different from the gradually transitioning boundaries commonly observed in VMS-type deposits.
	A copper-mineralized slate fragment and breccias within a single orebody			This new observation indicates that the copper mineralization post-dates the Lower Permian slate, and part of the copper mineralization, consider secondary remobilization.
	A saw-toothed boundary between copper ore and the wall rocks			It indicates the orebody was controlled by faults.
	Copper ore veinlets and malachite mineralization in the wall rock			It implies hydrothermal fluids filled the secondary structures.
	The striations and step surfaces to the copper orebodies			It indicates that the ore-controlling structures were thrust faults.
	The presence of quartz veins in the hanging wall			
Conjugate joint	The wall rocks were affected by compressions along both N-S and SW.			NW-striking faults may result from compression along the SW in response to the Indosinian closure event.
	Copper orebodies by compression along N-S.			The post-mineralization, NE-striking faults is likely the result of compression along N-S, related to the subsequent Himalayan collision.

faults in both ophiolites and slates (Table 3). In addition, orebodies were found in gabbro at the Changmahe mineral occurrence, limestone at the Qienugou mineral occurrence, the contact zone between granite and slate at the Zhaheleigou mineral occurrence and volcanic rocks at the Renguoshan mineral occurrence (Duan, 1998). This indicates that the Deerni copper deposit is not exclusively associated with ophiolite but is also controlled by faults.

The copper orebodies of the Deerni deposit are hosted in both brecciated ophiolite and early Permian slate (Fig. 5a and b). These orebodies strike NW and dip moderately to the northeast (Fig. 5a), displaying clear boundaries with the wall rocks (Table 4). Layered carbonate occurs between the orebody and the wall rocks. The Deerni copper deposit was controlled by faults, evidenced by (1) the presence of copper-mineralized slate fragments and breccias within a single orebody (Fig. 5c), (2) a saw-toothed boundary between copper ore and the wall rocks and (3) copper ore veinlets and malachite mineralization in the wall rock. The striations and step surfaces on the copper orebodies, alongside quartz veins in the hanging wall, suggest that the ore-controlling structures are thrust faults (Fig. 5d).

Near the No. 2 orebody, a statistical study of the conjugate joint sets in both the wall rocks and the copper orebodies involved analyzing 300 jointed fabrics to determine the direction of compression. The attitudes of fractures associated with all structural stages were measured and plotted on stereographic projections (Fig. 5e and f). The results indicate that the wall rocks

https://doi.org/10.1017/S0016756825100083 Published online by Cambridge University Press

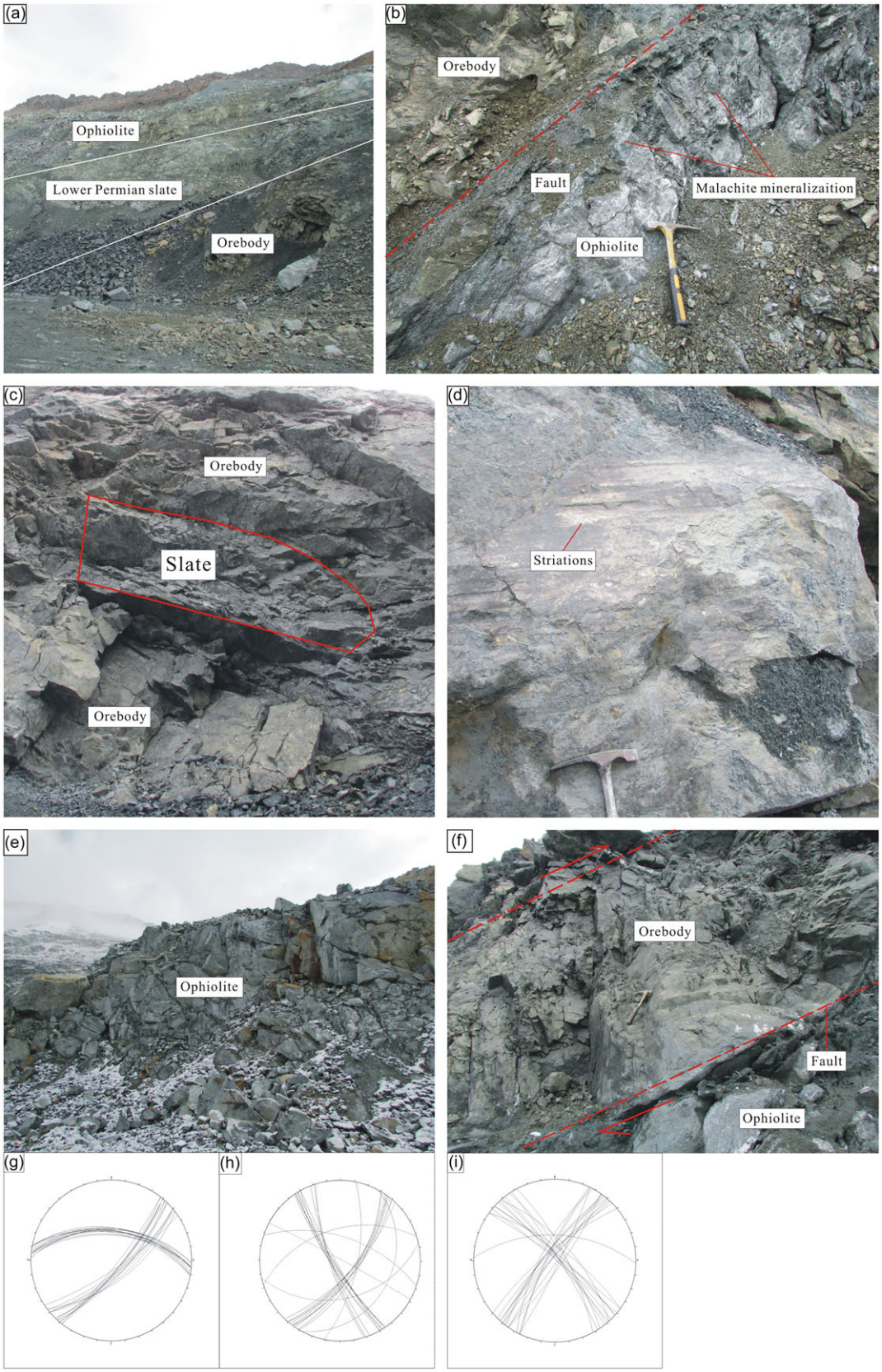

Figure 5. Field relations for the faulted contact between the copper orebodies and wall rocks at the Deerni copper deposit: (a) The Lower Permian slate forming the hanging wall to the copper orebodies; (b) The ophiolite footwall affected by malachite mineralization; (c) A copper-mineralized slate fragment within a copper orebody; (d) Striations on the surface of strata within the copper orebodies; (e) The attitudes of fractures associated with all structural stages were measured in the wall rocks and plotted on stereographic projections; (f) The attitudes of fractures associated with all structural stages were measured in the copper orebodies and plotted on stereographic projections; (g, h) The compression direction occurring in the wall rocks; (i) The compression direction of the copper orebodies.

https://doi.org/10.1017/S0016756825100083 Published online by Cambridge University Press

Table 4. The Deerni copper deposit comparing with the Yangla copper deposit

	Deerni copper deposit	Yangla copper deposit
Wall rocks	ophiolite, slate	sandstone, marble, sericitic slate and granodiorite
Morphology of orebody	lenticular	lenticular
Structures	compact massive, disseminated, brecciated and veinlet	compact massive structure, disseminated structure and veinlet
Ore minerals	pyrite, chalcopyrite, sphalerite, pyrrhotite and magnetite	pyrite, chalcopyrite, pyrrhotite, bornite, chalcocite, galena, sphalerite and magnetite
Elements combination	Cu、 Co、 Zn、 Au、 Ag	Cu、Pb, Zn, Au, Ag
Wall rock alteration	serpentinization, carbonatization, silicification, magnetite mineralization and malachite alteration	silicification, magnetite mineralization and malachite alteration
$\delta^{34}S$ values of sulphides	–6.2‰ to 6.6‰ (Zhang & Li, 2019)	–6.9‰ to 2.5‰ (Pan *et al.* 2012)
Ore-controlling faults	NW trending thrust faults	N-S trending thrust faults
Ore-forming age	There is no direct data for the Deerni deposit. The formation of ore deposits in the Eastern Kunlun Mountains is at 240–217 Ma (Feng *et al.* 2009, 2011; He *et al.* 2009; Wang *et al.* 2013)	^{187}Re-^{187}Os isochron age of 233.3 ±3 Ma (Yang *et al.* 2012)
The age of magmatic rocks	Zircon SHRIMP U-Pb age of the Deqia granitic complex is at 250 ± 20 Ma (Yang *et al.* 2005)	zircon U–Pb age of the granitoid is at 234.1 ± 1.2 to 235.6 ±1.2 Ma (Yang *et al.* 2013)
Metallogenic belt	Tethys metallogenic belt	Tethys metallogenic belt

experienced compression along both N-S and SW directions (Fig. 5g and h), and the copper orebodies were predominantly affected by compression along the N-S direction (Fig. 5i).

4.c. Distribution of copper mineralization

A total of 923 samples were collected from drill cores in the western part of Deerni. The spacing of exploration lines was set at 100 m, with varying depths below the surface ranging from 4471 to 3906 m (Fig. 6a and b).

5. Discussion

5.a. Proposed model for the Deerni copper mineralization

The boundary between the orebodies and the wall rocks at the Deerni deposit is sharp, contrasting with the gradual transitions typically observed in VMS deposits (Galley *et al.* 2007). The hanging wall of the copper orebodies is composed of slate (Fig. 5a), which has undergone silicification and extensive sub-parallel shear fracturing. The footwall is made up of ophiolite, affected by malachite mineralization (Fig. 5b). As a result, the ophiolite serves as the host rock for the copper orebody, overlain by slate.

The Deerni copper deposit is located within the anticlinal core and hosted within the NW-striking faults. This indicates that the Deerni copper deposit was mainly controlled by the NW-striking faults that overprinted the anticline (Figs. 1c and 2). Both the Deerni copper deposit and the Deqia granitic complex, located within the anticlinal core (Fig. 1c), suggest that they are potentially also temporally and genetically related. This is supported by the following evidence. (1) The Yangla copper deposit and the Deerni copper deposit are both located within the Tethys metallogenic belt (Table 4). Recent studies suggest that the Yangla copper deposit is related to the Yangla granodiorite, rejecting its previous classification as a VMS-type deposit (Yang *et al.* 2011, 2012; Chen *et al.* 2013; Yang *et al.* 2014*b*; Wei *et al.* 1999). The $\delta^{34}S$ values of sulphides from the Deerni deposit (–6.2 ‰ to 6.6 ‰) (Zhang & Li, 2019) are similar to those from the Yangla copper deposit (–6.9 ‰ to 2.5 ‰) (Pan *et al.* 2012), suggesting a similar genesis associated with nearby granitoids (Zhang & Li, 2019). (2) The $\delta^{65}Cu$ values from the Deerni deposit (–0.89 ‰ to –0.29 ‰) (Li *et al.* 2014) are consistent with those from magmatic deposits and igneous rocks, further supporting a magmatic origin (Li *et al.* 2014; Ikehata & Hirata, 2012; Zhou *et al.* 2013; Zhao *et al.* 2017). (3) The upper parts of the copper orebodies have higher concentrations of Zn, Gd and Ga, and lower concentrations of Co and In, showing a typical magmatic-hydrothermal metallogenic zoning pattern (Duan, 1998). (4) The age of formation of copper deposits in the Eastern Kunlun Mountains (240–217 Ma) coincides with the emplacement of Indosinian granitoids, highlighting a close spatial and temporal relationship (Feng *et al.* 2009, 2011; He *et al.* 2009; Wang *et al.* 2013). The Deerni copper deposit's genesis is likely related to the Indosinian granitoids, dated at ~250 Ma, located to the north of the deposit (Xia *et al.* 2015).

The Deqia granitic complex was formed around 250 ± 20 Ma (SHRIMP U-Pb zircon age; Yang *et al.* 2005), indicating that the Deerni copper deposit and the complex likely formed during the closure of the proto-Tethyan Ocean between 250 and 220 Ma (Yang *et al.* 2013, 2014*a*, 2014*b*; Li *et al.* 2018). The NW-trending Deqia granitic complex intruded along the NW-striking faults, with its eastern part cut by a NE-striking fault, and the deposit is intersected by a NE-striking fault (Fig. 2). Thus, both the Deerni copper deposit and the Deqia granitic complex postdate the NW-striking faults and predate the NE-striking faults.

Two stages of tectonic activity in the Deerni area likely correspond to regional tectonic events. The deposit is located within the Animaqin tectonic belt, which experienced the closure of the proto-Tethyan Ocean during the Indosinian orogeny and the subsequent India-Eurasia collision during the Himalayan Orogeny (Bi *et al.* 1999). The pre-mineralization NW-striking faults likely resulted from southwest-directed compression associated with the Indosinian closure. Post-mineralization NE-striking faults likely formed from north-south compression linked to the subsequent Himalayan collision (Patriat & Achache, 1984; Chen *et al.* 2000*b*; Bouilho *et al.* 2013; Gibbons *et al.* 2015).

The malachite mineralization, characteristic of the supergene stage, postdates silicification and magnetite mineralization. Pre-existing fractures in the Late Carboniferous ophiolitic strata and Lower Permian slate likely provided conduits for these fluids, leading to fluid-rock interactions that played a key role in copper mineralization, suggesting that the copper mineralization post-dated structural activity affecting the Lower Permian strata in the region.

https://doi.org/10.1017/S0016756825100083 Published online by Cambridge University Press

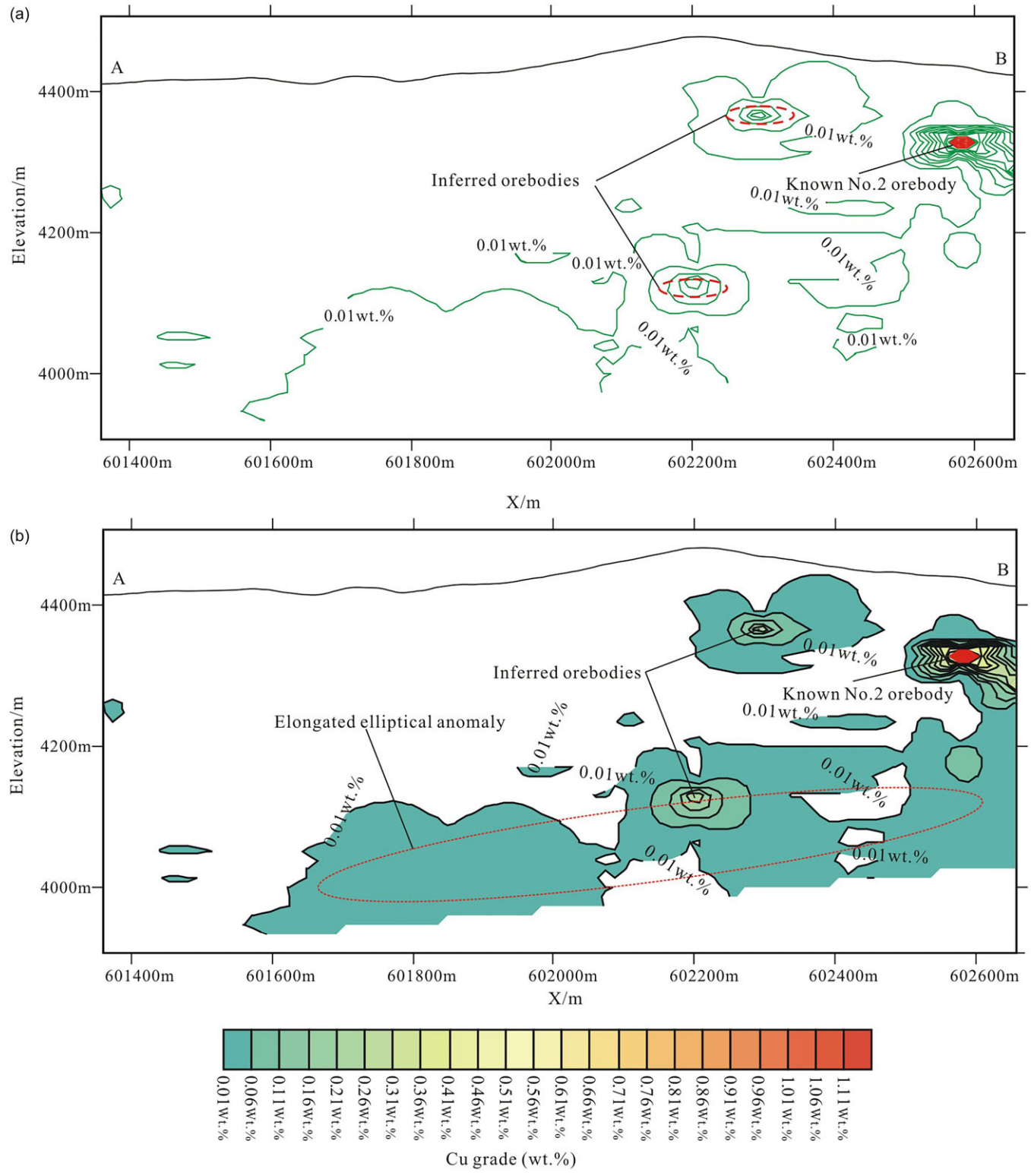

Figure 6. (a) Distribution pattern of copper mineralization in the longitudinal projection of the western part of the Deerni copper deposit. One copper anomaly occurs surrounding the No. 2 copper orebody, and two anomalies are distributed in the western part of the No. 2 copper orebody. (b) Surface trend diagrams of the copper mineralization in the longitudinal projection of the western part of the Deerni copper deposit. A linear low-grade area beneath the No. 2 orebody extends ~1 km to the west.

5.b. Exploration areas

Our study indicates that additional concealed copper orebodies are likely located beneath the silicified caps in both the eastern and western regions of the Deerni copper deposit. Observations from the No. 1 orebody suggest that these orebodies extend eastward, although they are intersected by a normal fault (Fig. 2). However, the depth of these concealed orebodies, ~300 meters, makes them unsuitable for open-pit mining. Observations from the western Deerni suggest that these concealed copper orebodies may be an

https://doi.org/10.1017/S0016756825100083 Published online by Cambridge University Press

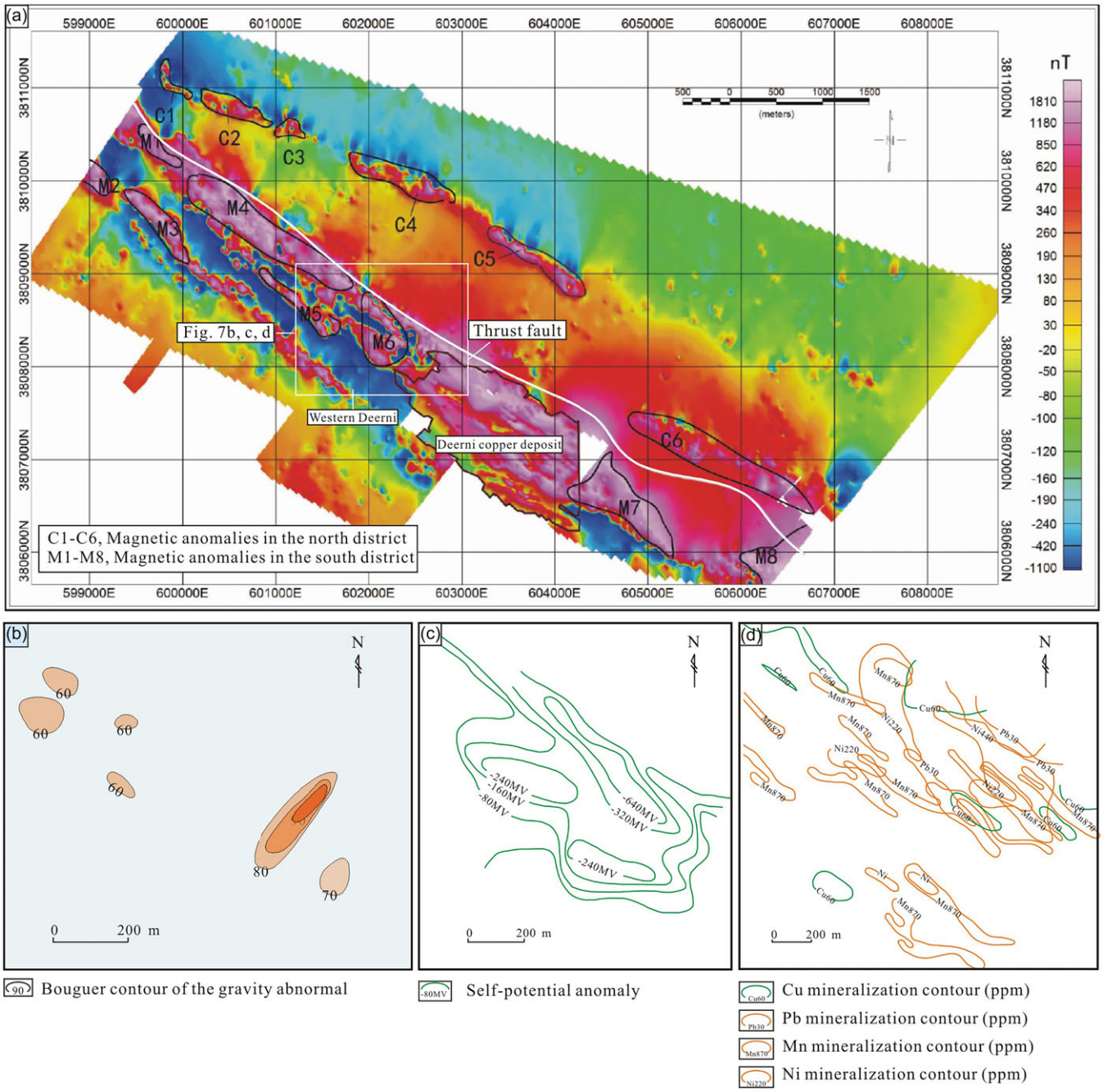

Figure 7. (a) Magnetic anomaly pattern for the western Deerni orebodies; (b) Gravity anomaly pattern for the western Deerni orebodies; (c) Self-potential anomaly pattern at western Deerni; (d) Distribution pattern of Cu–Pb–Mn–Ni mineralization for western Deerni (Liu *et al.* 2019; based on unpublished data from the Zijin Mining Group Company Limited).

extension of the No. 2 orebody (Fig. 2). The prediction has been verified by geophysical and geochemical methods.

Xue (1992) and Liu *et al.* (2019) suggested that magnetic anomalies can be used to detect copper orebodies at the Deerni copper deposit due to the significant difference in magnetic susceptibility between the copper orebodies and the surrounding ophiolitic wall rocks [mean value of 10,400 vs. 310–1100 ($4\pi \cdot 10^{-6}$ SI)]. A series of strong magnetic anomalies were detected in the Deerni copper area (Fig. 7a, Zijin Mining Group Co., Ltd). The strong magnetic anomalies are perfectly aligned with the NW-SE-trending fault zone. Since the Deerni copper deposit was controlled by the NW-SE trending fault zone, the strong magnetic anomalies are likely caused by either strongly magnetic rocks in the NW-SE-trending fault zone or ore-bearing formations (Holden *et al.* 2012; Kwan *et al.* 2025). Comparing the magnetic anomalies with the known Cu orebodies at the Deerni copper deposit, it is clear that the anomalies are not associated with Cu orebodies, but with the ophiolitic host (DeMatties, 2024).

Wang *et al.* (2007*a*) suggests that gravity anomalies can effectively identify copper deposits at Deerni due to the density contrast between the copper orebodies (4.52–4.88 g/cm^3, average of 4.66 g/cm^3) and the surrounding wall rocks (ophiolite and slate, 2.60–2.80 g/cm^3) Current mining areas (hosting orebodies No. 1, 2 and 5) all correspond to zones of high positive gravity anomalies

https://doi.org/10.1017/S0016756825100083 Published online by Cambridge University Press

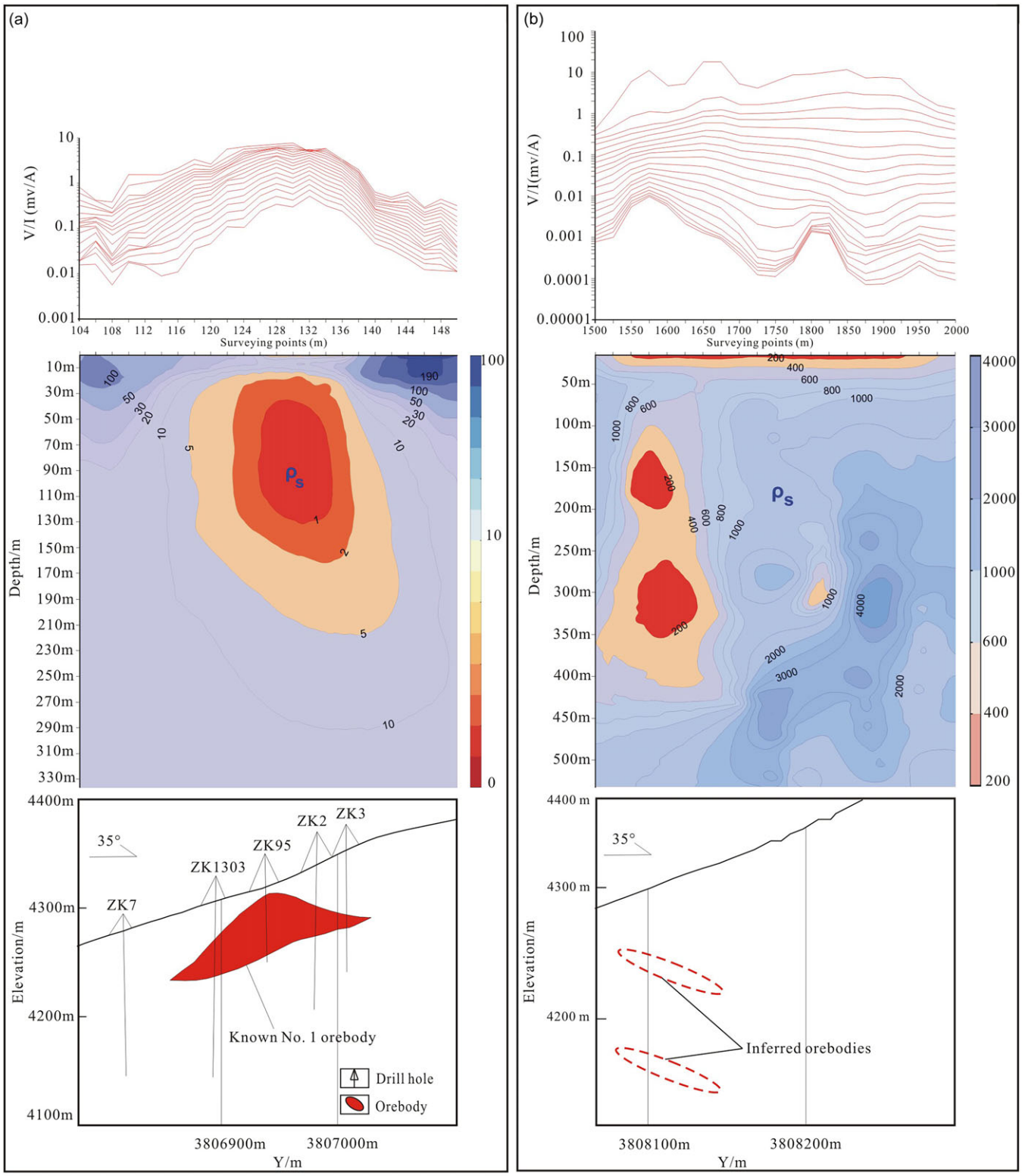

Figure 8. Transient electromagnetic anomaly profile at Deerni copper deposit. (a) Transient electromagnetic anomaly profile along exploration Line 13 of the Deerni copper deposit; (b) Transient electromagnetic anomaly profile along Line 3 at the western Deerni (based on unpublished data from the Zijin Mining Group Company Limited).

(Wang *et al.* 2007*a*). A positive gravity anomaly was also detected in western Deerni (Fig. 7b, Zijin Mining Group Co., Ltd), extending south-westward, with a length of ~750 m, a width of ~250 m, and covering an area of ~0.19 km^2. The maximum anomaly (>90×10 m/s^2) is located at the northeast end. However, the anomaly's orientation does not align with the dip or strike of the No. 2 orebody, indicating that it may be caused by the surrounding wall rocks or other ore-bearing formations.

Wang *et al.* (2007*b*) suggested that self-potential anomalies are an effective tool for locating concealed orebodies as copper ores in

https://doi.org/10.1017/S0016756825100083 Published online by Cambridge University Press

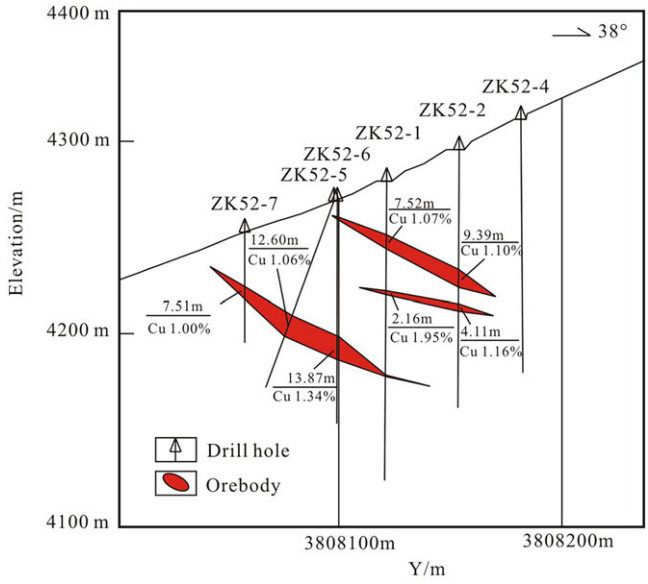

Figure 9. Cross-section 52 through western Deerni and its orebodies (based on unpublished data from the Zijin Mining Group Company Limited).

the Deerni deposit contain sulphides. The sulphides significantly increase the electrical conductivity of the ore rocks (10^{-4} Ω·m) to be several times higher than that of the wall rocks. The known mining areas (orebodies No. 1, No. 2 and No. 5) lie within high self-potential anomaly zones (Wang *et al.* 2007*b*; Liu *et al.* 2010; Zhang, 2014). In the northwest and central parts of western Deerni, three negative self-potential anomalies were identified (Fig. 7c, Zijin Mining Group Co., Ltd). The first anomaly is elliptical with a northwest-southeast axis, measuring 330 m in length, 100 m in width and covering an area of 0.03 km^2, with a maximum amplitude of −240 mV. The second extends north-westward, measuring ~800 m by ~100 m, covering ~0.08 km^2, with a maximum amplitude of −640 mV. The third anomaly forms a belt, extending north-westward over 300 m, covering 0.03 km^2, with an amplitude of more than −240 mV. The self-potential anomalies align with the strike of the No. 2 orebody, suggesting they are caused by either the orebody itself or nearby concealed copper orebodies.

The No. 1 orebody is located at 20 m below the surface, and the No. 1 orebody generated one transient electromagnetic anomaly 50 m below the surface (Fig. 8a, Zijin Mining Group Co., Ltd). On the transient electromagnetic anomaly profile of western Deerni, two anomalies were detected (Fig. 8b, Zijin Mining Group Co., Ltd). Two deeper anomalies are located at 150 and 300 m below the surface, suggesting that they are likely caused by concealed copper orebodies (Xue *et al.* 2024).

The Cu grade contour diagram (Fig. 6a) reveals relatively ordered isolines for three Cu anomalies. One Cu anomaly surrounds the No. 2 copper orebody, and two additional Cu anomalies are distributed in the western part of this orebody. One surrounds the No. 2 orebody, confirming its association with this orebody. Two additional anomalies are found west of the No. 2 orebody, suggesting the presence of concealed orebodies at depths of 150 and 300 m. These anomalies correspond to the transient electromagnetic anomalies, reinforcing the likelihood of concealed copper deposits in the west of the No. 2 orebody. On the surface trend diagrams of copper mineralization (Fig. 6b), in addition to the three Cu anomalies, an elongated elliptical anomaly with low Cu grades was identified. This elongated elliptical anomaly is located beneath the No. 2 orebody and extends ~1 km to the west, between elevations of 4200–4000 m, indicating a low-Cu-grade belt extending 1 km westward beneath the No. 2 orebody. Geochemical anomalies for Cu, Pb, Mn and Ni mineralization were identified in western Deerni (Fig. 7d, Zijin Mining Group Co., Ltd). The Cu anomalies overlap with Mn anomalies, extending along the strike and dip of the No. 2 orebody. The Cu anomalies largely coincide with the self-potential anomalies in western Deerni (Fig. 7c, Zijin Mining Group Co., Ltd). Collectively, geological, geophysical and geochemical data point to the presence of concealed copper deposits in western Deerni.

5.c. Drill test results

In the new drilling holes completed at the western Deerni area, concealed copper orebodies were discovered and contributed to the total copper reserve of the deposit. In the number 52 cross-section through western Deerni (Fig. 9), three concealed orebodies were discovered, which are 7.15–13.87 m wide with Cu grade between 1.00 and 1.34 wt.%., adding >10,000 tonnes to the Cu reserve at Deerni. We thus confirm that they represent the westward extension of the No. 2 orebody in the east. Therefore, the copper orebodies at the Deerni deposit are controlled by structures, and the silicified cap of earthy yellow crust at the ground surface is an effective indicator of copper mineralization underground, analogous to a gossan.

6. Conclusions

(1) The Deerni copper deposit is controlled by the NW-striking faults. Serpentinization, carbonatization, silicification, malachite alteration and magnetite mineralization have occurred along fractures within the wall rocks and surrounding strata, suggesting that this alteration post-dated structural activity affecting the Lower Permian strata in the region.

(2) Field investigations, geophysical and geochemical data suggest the presence of copper orebodies in western Deerni.

(3) The drilling holes intercepted the concealed copper orebodies in the western Deerni area and significantly enhanced the copper reserve at the Deerni deposit.

Acknowledgements. This study was financially supported by the National Natural Science Foundation of China (No. 41830430). We would like to express our gratitude to Wankun Li, Baowen Yan and others for providing geological data and for their assistance and hospitality during fieldwork at the Deerni copper deposit and surrounding areas. We are deeply indebted to Professor Guoxiang Chi for his incisive reviews, valuable comments and suggestions that significantly improved an earlier draft of this manuscript. The authors would also like to thank the associate editor, Dr. Simon Schorn, and anonymous reviewers for their constructive comments, which significantly improved the manuscript.

References

Bi H, Wang Z, Wang Y and Zhu X (1999) History of tectono-magmatic evolution in the Western Kunlun Orogen. *Science in China Series D: Earth Sciences* **42**, 604–19.

Bouilho LP, Jagoutz O, Hanchar JM and Dudas FO (2013) Dating the India–Eurasia collision through arc magmatic records. *Earth and Planetary Science Letters* **366**, 163–75.

Chen L, Sun Y, Liu XM and Pei XZ (2000a) Geochemistry of Derni ophiolite and its tectonic significance. *Acta Petrologica Sinica* **16**, 106–10.

https://doi.org/10.1017/S0016756825100083 Published online by Cambridge University Press

Chen L, Sun Y, Pei X, Feng T and Zhang G, (2004) Comparison of eastern paleo-Tethyan ophiolites and its geodynamic significance. *Science in China Series D-Earth Sciences* **47**, 378–384.

Chen L, Sun Y and Pei XZ (1999) Derni Ophiolite: northernmost Tethyan lithosphere relics in Tibet Plateau. *Journal of Northwest University (Natural Science Edition)* **29**, 141–44.

Chen L, Sun Y, Pei XZ, Gao M, Feng T, Zhang ZQ and Chen W (2001) 40Ar–39Ar dating of Derni ophiolite: evidence from the existence and stretch of Paleotethys in the northern Tibetan Plateau. *Chinese Science Bulletin* **46**, 424–26 (in Chinese).

Chen SY, Gu XX, Cheng WB, Zheng L, Han SY and Peng YW (2013) Characteristics of ore-forming fluid and mineralization process of Yangla copper deposit, Yunnan. *Earth Science Frontiers* **20**, 82–91 (in Chinese with English abstract).

Chen ZH, Burchfiel BC, Liu Y, King RW, Royden LH and Tang W (2000b) Global Positioning System measurements from eastern Tibet and their implications for India/Eurasia intercontinental deformation. *Journal of Geophysical Research: Solid Earth* **105**, 16215–27.

DeMatties TA (2024) Reassessment of the Big Mike copper–cobalt volcanogenic massive sulphide deposits (VMS): implications for further exploration in the Late Paleozoic Havallah Ophiolite Sequence, north-central Nevada, USA. *International Journal of Earth Science and Geophysics* **10**, 074.

Duan GL (1991) The Derni pyrite type Cu–Co deposit: its genesis and difference from Cu–Ni sulphide deposits. *Geology and Prospecting* **27**, 20–24 (in Chinese with English abstract).

Duan GL (1996) Metallogenetic regularity of the pyrite-type copper/cobalt deposit in De'erni region. *Geology of Chemical Minerals* **18**, 92–100 (in Chinese with English abstract).

Duan GL (1998) Geological characteristics of De'erni pyrite-type copper/cobalt deposit and its difference from Cyprus copper deposit. *Geology of Chemical Minerals* **20**, 287–94 (in Chinese with English abstract).

Duan J, Qian ZZ, Huang XF, Dong FQ, Zhao XJ and Lu H (2014) Characteristics of ore minerals of De'erni Cu (Co) deposit in Qinghai and their geological significance. *Journal of Earth Sciences & Environment* **36**, 201–209.

Feng CY, Li DS, Qu WJ, Du AD, Wang S, Su SS and Jiang JH (2009) Re–Os isotopic dating of molybdenite from the Suolajier skarn-type copper–molybdenum deposit of Qimantage Mountain in Qinghai Province and its geological significance. *Rock and Mineral Analysis* **28**, 223–27 (in Chinese with English abstract).

Feng CY, Wang XP, Shu XF, Zhang AK, Xiao Y, Liu JN and Ma SC (2011) Isotopic chronology of the Hutouya skarn lead–zinc polymetallic ore district in Qimantage area of Qinghai Province and its geological significance. *Journal of Jilin University (Earth Science Edition)* **41**, 1806–17 (in Chinese with English abstract).

Galley AG, Hannington MD and Jonasson IR (2007) Volcanogenic massive sulphide deposits. *Mineral Deposits of Canada: A Synthesis of Major Deposit-Types, District Metallogeny, the Evolution of Geological Provinces, and Exploration Methods* **5**, 141–61.

Gibbons AD, Zahirovic S, Müller RD, Whittaker JM and Yatheesh V (2015) A tectonic model reconciling evidence for the collisions between India, Eurasia and intra-oceanic arcs of the central-eastern Tethys. *Gondwana Research* **28**, 451–92.

Guo X, Zhou T, Fan Y, Wang F, Liu Z and Zhu X (2024) Cobalt occurrence and sulfide geochemistry of the De'erni Cu–Zn–Co deposit in NW China. *Ore Geology Reviews* **172**, 106218.

He SY, Li DS, Li LL, Qi LY and He SF (2009) Re–Os age of molybdenite from the Yazigou copper (molybdenum) mineralized area in eastern Kunlun of Qinghai Province, and its geological significance. *Geotectonica et Metallogenia* **33**, 236–42 (in Chinese with English abstract).

Holden E-J, Wong JC, Kovesi P, Wedge D, Dentith M and Bagas L (2012) Identifying structural complexity in aeromagnetic data: an image analysis approach to greenfields gold exploration. *Ore Geology Reviews* **46**, 47–59.

Ikehata K and Hirata T (2012) Copper isotope characteristics of copper-rich minerals from the Horoman peridotite complex, Hokkaido, northern Japan. *Economic Geology* **107**, 1489–97.

Jiao JG, Huang XF and Yuan HC (2009) Progress in the research of De'erni Cu (Co) ore deposit. *Journal Science and Environment* **31**, 42–47 (in Chinese with English abstract).

Kwan K, Müller D, Groves DI, Legault JM, Reford S, Maacha L, Ouadjou A, Cao YW and Liu J (2025) The S3 orogenic gold targeting algorithm: a case study from the Timmins gold camp, Ontario, Canada. *Geophysics* **90**, 1–16.

Li S, Zhao S, Liu X, Cao H, Yu S, Li X and Suo Y (2018) Closure of the Proto-Tethys Ocean and Early Paleozoic amalgamation of microcontinental blocks in East Asia. *Earth-Science Reviews* **186**, 37–75.

Li XH, Chu FY and Lei JJ (2014) The copper isotopic composition of sulfide ores and deposit genesis of the Dur'ngoi Cu (Zn–Co) deposit in Qinghai Province, China. *Earth Science Frontiers* **21**, 196–204 (in Chinese with English abstract).

Liu JL, Xu XX, Wang K, Zhang W and Cai SF (2010) Study of integrated geophysical survey method used for peripheral region of De'erni cobalt–copper ore deposit. *Northwestern Geology* **43**, 70–79 (in Chinese with English abstract).

Liu JW, Peng XF, Wang T, Wang XM and Zhang KN (2019) Qinghai Del copper mine geological characteristics and optimization of peripheral target. *Mineral Exploration* **10**, 1113–18 (in Chinese with English abstract).

Liu ZY, Liu CM and Shi CY (2007) Regional geochemical anomalous characteristics criteria for ore prospecting of the Dur'ngoi hydrothermal Cu–Co deposit in Qinghai. *Computing Techniques for Geophysical and Geochemical Exploration* **29**(S1), 184–88 (in Chinese with English abstract).

Pan G, Wang L, Li R, Yuan S, Ji W, Yin F and Wang B (2012) Tectonic evolution of the Qinghai–Tibet Plateau. *Journal of Asian Earth Sciences* **53**, 3–14.

Patriat P and Achache J (1984) India–Eurasia collision chronology has implications for crustal shortening and driving mechanism of plates. *Nature* **311**, 615–21.

Song ZB, Chen XY and Ren YX (2008) Petroregimentation, petrochemistry and geological meaning of "Carbonaceous (Gritstone) slabstone" in De'erni deposit, eastern Kunlun Area, northwest China. *Northwest Geology* **41**, 77–81 (in Chinese with English abstract).

Song ZB, Li YZ and Chen XY (2012) Discovery of exhalative rock ferro-siliceous rock in the De'erni copper deposit of eastern Kunlun Mountains and its metallogenic significance. *Geological Bulletin of China* **31**, 1170–77. (In Chinese with English abstract).

Song ZB, Wang X, Ren YX and Li YZ (2007). Superimposed mineralization of Deerni Co-Cu deposit, East Kunlun Mountains, NW China. *Northwest Geology* **40**, 1–6 (in Chinese with English abstract).

Tang D, Qin K and Mao Y (2024) Source of metals in the De'erni ultramafic-hosted volcanic massive sulfide deposit, Eastern Kunlun, China. *Miner Deposita* **59**, 1207–27.

Wang FC, Chen J, Xie Z, Li SP, Tan SX, Zhang YB and Wang T (2013) Geological features and Re–Os isotopic dating of the Lalingzaohuo molybdenum polymetallic deposit in East Kunlun. *Geology in China* **40**, 1209–17. (In Chinese with English abstract).

Wang K, Chen XY, Wang YX and Lu XC (2007a) Optimum method of geophysical exploration for De'erni cobalt–copper ore deposit. *Gansu Metallurgy* **16**, 79–85. (In Chinese with English abstract).

Wang K, Liu KH, Geng T and Lv XC (2007b) Abnormity characteristics of SP method and significance of ore prospecting in Dererny Mining Area and its periphery. *Gansu Metallurgy* **29**, 25–32 (In Chinese with English abstract).

Wang K, Lu XC, Zhao JM, Chen B and Chen XY (2008) The application of the transient electromagnetic method to numerical calculation and field test of the De'erni cobalt–copper ore deposit. *Geophysical and Geochemical Exploration* **32**, 366–69. (In Chinese with English abstract).

Wang ZT and Qin KZ (1989) Types of metallogenic environments and characteristics of temporal and spatial distribution of copper deposits in China. *Acta Geologica Sinica* **2**, 79–92.

Wei JQ, Chen KX and He LQ (1999) A discussion on the structural environment for forming the volcanic rock in Yangla region. *Yunnan Geology* **18**, 53–62. (In Chinese with English abstract).

Xia R, Wang C, Qing M, Deng J, Carranza EJM, Li W and Yu W (2015) Molybdenite Re–Os, zircon U–Pb dating and Hf isotopic analysis of the Shuangqing Fe–Pb–Zn–Cu skarn deposit, East Kunlun Mountains, Qinghai Province, China. *Ore Geology Reviews* **66**, 114–31.

Xue GQ, Zhou N, Su BX, Zhang AK, Yang YC, Mo JP and Wu X (2024) Geophysical exploration strategy for Cu–Ni–Co deposits in China: a review. *Geophysics* **89**, WB25–34.

Xue GR (1992) Geological–geophysical–geochemical model of the Deerni copper–cobalt, Qinghai Province. *Qinghai Geology* **2**, 81–95 (In Chinese with English abstract).

Yang J, Shi R, Wu C, Wang X and Robinson PT (2009) Dur'ngoi ophiolite in East Kunlun, Northeast Tibetan Plateau: evidence for paleo-Tethyan suture in Northwest China. *Journal of Earth Science* **20**, 303–31.

Yang JS, Xu ZQ and Li HB (2005) The Paleo-Tethyan volcanism and plate tectonic regime in the A'nyemaqen region of East Kunlun, Northern Tibet Plateau. *Acta Petrologica et Mineralogica* **24**, 369–80 (In Chinese with English abstract).

Yang XA, Liu JJ, Cao Y, Han SY, Gao BY, Wang H and Liu YD (2012) Geochemistry and S, Pb isotope of the Yangla copper deposit, Western Yunnan, China: implication for ore genesis. *Lithos* **144**, 231–40.

Yang XA, Liu JJ, Han SY, Jiang GH and Zhai DG (2014b) Isotope geochemistry and its implications in the origin of Yangla copper deposit, Western Yunnan, China. *Geochemical Journal* **48**, 19–28.

Yang XA, Liu JJ, Han SY, Zhang HY, Luo C, Wang H and Chen SY (2011) U–Pb dating of zircon from the Linong granodiorite, Re–Os dating of molybdenite from the ore body, and their geological significances in Yangla copper deposit, Yunnan. *Acta Petrologica Sinica* **27**, 2567–76 (In Chinese with English abstract).

Yang XA, Liu JJ, Li DP, Zhai DG, Yang LB and Han SY (2013) Zircon U–Pb dating and geochemistry of the Linong granitoid and its relationship to Cu mineralization in the Yangla copper deposit, Yunnan, China. *Resource Geology* **63**, 224–38.

Yang XA, Liu JJ, Yang LB, Han SY, Sun XM and Wang H (2014a) Fluid inclusion and isotope geochemistry of the Yangla copper deposit, Yunnan, China. *Mineralogy and Petrology* **108**, 303–15.

Yang XA, Wu J, Coulson IM, Zhang JZ, Lai XD, Zhang YB and Xu DR (2020) Discovery of concealed ore-bodies at the Dongping gold deposit, Northern China, revealed by the study of ore-controlling structures. *Ore Geology Reviews* **118**, 103216.

Yang XA, Wu J, Xu DR and Ren HB (2023) Application of integrated geological and structural investigations to the discovery of new mineral zones related to the Daping gold deposit, Southwest China. *Ore Geology Reviews* **158**, 105519.

Zhang CZ (2014) The exploring history of the Deerni copper deposit in the Guoluo County. *Geophysical & Geochemical Exploration* **38**, 1095–96 (In Chinese).

Zhang HT and Li JH (2019) Impacts of serpentinization on ultramafic rock-hosted hydrothermal system along mid-ocean ridges: insight from Dur'ngoi copper massive sulfide deposit, Tibetan Plateau. *Geotectonica et Metallogenia* **43**, 111–22.

Zhang WS (1995) A specific type of massive sulphide deposits De'erni copper deposit. *Acta Geologica Gansu* **4**, 22–31 (In Chinese with English abstract).

Zhang WS, Chen J (1996) New recognition on the origin of the De'erni copper deposit: A Cu-Co bearing massive sulfide deposit in ultrabasic rocks. *Qinghai Geology* **1**, 37–52 (In Chinese with English abstract).

Zhao G and Guo J (2012) Precambrian geology of China: preface. *Precambrian Research* **222–223**, 1–12.

Zhao Y, Xue C, Liu SA, Symons DT, Zhao X, Yang Y and Ke J (2017) Copper isotope fractionation during sulfide–magma differentiation in the Tulaergen magmatic Ni–Cu deposit, NW China. *Lithos* **286**, 206–15.

Zhou JX, Wang JS, Yang DZ and Liu JH (2013) H–O–S–Cu–Pb isotopic constraints on the origin of the Nage Cu–Pb deposit, Southeast Guizhou Province, SW China. *Acta Geologica Sinica-English Edition* **87**, 1334–43.

https://doi.org/10.1017/S0016756825100083 Published online by Cambridge University Press